J. Fluid Mech. (1986), *vol.* 166, *pp.* 189–209
Printed in Great Britain

Interactions among multiple three-dimensional bodies in water waves: an exact algebraic method

By HIROSHI KAGEMOTO† AND DICK K. P. YUE
Department of Ocean Engineering, Massachusetts Institute of Technology, Cambridge, Massachusetts

(Received 27 August 1984 and in revised form 19 November 1985)

We consider three-dimensional water-wave diffraction and radiation by a structure consisting of a number of separate (vertically) non-overlapping members in the context of linearized potential flow. An interaction theory is developed which solves the complete problem, predicting wave exciting forces, hydrodynamic coefficients and second-order drift forces, but is based algebraically on the diffraction characteristics of single members only. This method, which includes also the diffraction interaction of evanescent waves, is in principle exact (within the context of linearized theory) for otherwise arbitrary configurations and spacings. This is confirmed by a number of numerical examples and comparisons involving two or four axisymmetric legs, where full three-dimensional diffraction calculations for the entire structures are also performed using a hybrid element method. To demonstrate the efficacy of the interaction theory, we apply it finally to an array of 33 (3 by 11) composite cylindrical legs, where experimental data are available. The comparison with measurements shows reasonable agreement.

The present method is valid for a large class of arrays of arbitrary individual geometries, number and configuration of bodies with non-intersecting vertical projections. Its application should make it unnecessary to perform full diffraction computations for many multiple-member structures and arrays.

1. Introduction

With advances in the design and construction of large ocean structures, the problem of wave diffraction and radiation by an assembly of a number of bodies is becoming increasingly important. Large offshore platforms are now commonly designed with a composite configuration of several elemental members or legs such as cylinders or ellipsoids. Wave-power extraction studies have also pointed to the advantage of wave devices made up of an array of oscillating bodies (e.g. Budal 1977). A recent proposal in Japan (Ando, Okawa & Ueno 1983) for the construction of offshore floating airports and large storage facilities supported on many legs is another example where there is an immediate need for accurate and efficient theoretical predictions to supplement laboratory testing.

When a wave is incident on an array of bodies, it is necessary (except in some limiting cases) to account not only for the diffraction of each body by the incident field, but also the multiple scattering due to the other bodies. Thus each body diffracts waves towards the others, which in turn respond to this excitation and send back radiation that contributes to the total excitation of the original body, and so on. This concept of multiple scattering is common in all diffraction theories, and has appeared

† Present address: Ship Research Institute, Tokyo, Japan.

in the context of electromagnetic scattering in the literature since at least 1893 (see Heaviside 1950). For water waves the phenomenon is an aspect of hydrodynamic interaction and was first encountered in the study of pile arrays (Lebreton & Cormault 1969) and twin-hull vessels (Wang & Wahab 1970).

In principle, the full hydrodynamic interaction problem can be solved by performing a diffraction calculation for the entire ensemble as a unit, and a number of reliable numerical methods for this are now available (Mei 1978). Such computations, however, become prohibitive and infeasible as the number of members increase (similar difficulties are also encountered in designing suitably scaled experiments for these large structures). An attractive alternative is to require the diffraction solutions (theoretical or experimental) only for individual isolated members (they need not be identical) and to account for multiple scattering for an arbitrary configuration through some interaction theory that depends on these individual member properties only.

The first work in this direction appears to be that of Twersky (1952), who studied the two-dimensional scattering of acoustic radiation by an array of circular cylinders. He devised an iterative scheme in which more successive reflections among the cylinders were included at each higher order. Using an addition theorem for the cylindrical wave functions, the calculations were expedited by expressing the partial waves around one body in terms of those at the other cylinders. This idea was extended to surface waves by Ohkusu (1974), who applied it to a structure composed of three vertical circular cylinders. In neither case was convergence proven, although computational evidence in the latter and subsequent work using this method (e.g. Greenhow 1980; Duncan & Brown 1982) suggested that only a small number of iterations was in general required. The major drawback of these iterative methods is that, even for relatively low orders of approximation, the number of interacting wave components that must be accounted for increases rapidly and becomes intractable as the number of bodies increase.

Another approach is the direct matrix method, wherein the amplitudes of the wave components around each body is solved for simultaneously, subject to the boundary conditions of the respective bodies. This approach was considered by Spring & Monkmeyer (1974), although they only applied their analysis to the diffraction of uniform vertical cylinders that extend throughout the depth, thus avoiding the need for evanescent modes. More recently, Simon (1982) developed a plane-wave approximation in a direct matrix solution of a uniformly spaced linear array of axisymmetric bodies. This is strictly a large-spacing approximation, where by replacing the diverging waves at one body due to the scattering of another body by a single plane wave, a substantially simplified system can be obtained. The errors introduced, however, may not be insignificant (see §4). Simon applied his method to axisymmetric bodies in heaving motion only. McIver & Evans (1984) extended Simon's approach in their study of wave forces on arrays of fixed vertical circular cylinders. By including a correction term in the plane-wave approximation, they obtained greatly improved results over the latter, even when the body spacings are fairly small compared with the wavelength (cf. figure 3). This method has also been extended to the calculation of added mass and damping (McIver 1984) with equally satisfactory results for two floating cylindrical cylinders. Another interesting piece of work is that of Kyllingstad (1984), who, by further assuming that the bodies are small (compared with wavelength), obtained a low-scattering approximation in which the interaction forces can be expressed in terms of single body forces and hydrodynamic coefficients only.

With the exception of Ohkusu (1974), all of the above studies ignore the effect of the evanescent wavefield in the interaction consideration. This is based on the so-called wide-spacing approximation under which the amplitude of the local waves due to one body is assumed to be negligible at the neighbouring bodies. Thus, for typical body dimensions a and interbody spacing L, Srokosz & Evans (1979), for example, based this assumption on large spacing compared with wavelength λ, i.e. $k_0 L \gg 1$ ($k_0 = 2\pi/\lambda$). The other relevant parameter is clearly L/a. For fixed (but not small) values of L/a, the results of Srokosz & Evans for two vertical plates in two dimensions were remarkably good even for small $k_0 L$. Based on his numerical computations, Ohkusu (1974) proposed a criterion for neglecting local wave interactions that depended only on L/a (> 5 for the case of three symmetrically placed vertical cylinders). Martin (1984) performed a careful comparison between exact calculations and wide-spacing results for a pair of two-dimensional cylinders for a range of $k_0 a$ and L/a. The dependency of the error on $k_0 L$ is uneven in that for fixed L/a the results may or may not improve with increasing $k_0 L$, while for fixed $k_0 L$ there is a clear diminishing of the error when L/a becomes large. Martin concluded that both $k_0 L \gg 1$ and $L/a \gg 1$ are important for the wide-spacing approximation to be valid. Heuristically, when L/a is small enough, local standing waves must be important regardless of wavelength, while when $L/a \gg 1$ the overall interaction effects diminish accordingly, and the relative importance of evanescent waves is less clear. For finite water depth h our numerical results and a simple analysis (see §4) show that the more critical parameter is $(L-a)/h \gg 1$; and for fixed L/a and h/a evanescent wave interactions can in fact be more important for *shorter* waves. Although the wide-spacing approximation appears satisfactory for most applications, there exists little quantitative assessment of the importance of evanescent wave interactions for three-dimensional problems.

In this paper we present a new method for calculating the wave hydrodynamics of a multimember structure using the diffraction properties of individual members only. This procedure combines the features of the matrix method of Spring & Monkmeyer (1974) and Simon (1982) and the multiple-scattering technique of Twersky (1952) and Ohkusu (1974). Specifically, we represent the wavefield around each body as a series of partial waves of undetermined amplitudes. By applying a transformation to express the influence of the wave system at one body in terms of those at all the other bodies, a set of linear algebraic equations can be derived to satisfy the (given) diffraction characteristics of all the member bodies. This system is then solved simultaneously for all the unknown amplitude coefficients. To make the method general for arbitrary body spacings, we also include a system of local waves in the body wavefield representation. Thus, provided that an adequate number of terms are used, the final results are in fact *exact* in the context of linearized diffraction theory. Our present approach is applicable, with the exception of bodies having intersecting vertical projections,† to arbitrary body geometry, number and configuration, although calculations are simplified when the individual bodies are all axisymmetric.

As illustration, we present results for several different configurations of two and four floating or bottom-seated vertical cyclinders. To check our accuracy, 'exact' numerical results are obtained using a three-dimensional hybrid-element diffraction method (Yue, Chen & Mei 1978) which models the entire assembly as a whole. The comparisons are excellent in all cases for first-order quantities such as exciting forces

† Our use of the addition theorem for the cylindrical partial waves in fact imposes a somewhat stricter restriction on the geometry. See the discussion after (2.4).

and added-mass and damping coefficients, as well as for the second-order wave drift force. The results for steady drift are particularly significant since (i) mooring requirement is an important consideration for large multimember structures; (ii) as the number of legs become large, the total primary exciting force (per leg) diminishes for much of the frequency range owing to unequal incident phases at the individual members, while a corresponding implication for the steady drift force cannot be readily predicted; and (iii) relatively crude approximations can often produce surprisingly good predictions for first-order effects such as primary exciting forces; the small inaccuracies present can, however, lead to very large errors in the second-order drift-force calculations.

We remark that although the present method requires a larger number of unknowns (NM for N bodies and M average wave components per body) and fairly complete single-member diffraction information (including evanescent wave diffraction), compared with more approximate methods (such as Simon 1982), the total amount of effort needed is still very significantly less than that for a full diffraction calculation. Thus as a final example, we apply our theory to an array of 33 composite cylindrical legs that forms a portion of the support for a proposed floating airport, and for which experimental data are available. Our overall agreement with measurements is fairly satisfactory.

2. Formulation for an exact interaction theory

Consider the plane-wave diffraction (and radiation)† of an assembly of N floating three-dimensional bodies, under the usual assumption of linearized potential flow. We define local cylindrical coordinates (r_i, θ_i, z) fixed in the undisturbed free surface with the mean centre positions O_i of bodies $i = 1, 2, \ldots, N$ (see figure 1). Assuming a time factor $e^{-i\omega t}$ (for angular frequency ω, $\Phi(r, \theta, z, t) = \mathrm{Re}\,(\phi(r, \theta, z)\, e^{-i\omega t})$), the complex velocity potential representing the scattered wavefield *outside* an immediate neighborhood of body i (it is necessary to assume here that the bodies do not overlap vertically) can in general be expressed as a summation of cylindrical waves in that coordinate system:

$$\phi_i^S(r_i, \theta_i, z) = \frac{\cosh k_0(z+h)}{\cosh k_0 h} \sum_{n=-\infty}^{\infty} A_{on_i} H_n^{(1)}(k_0 r_i)\, e^{in\theta_i} + \sum_{m=1}^{\infty} \cos k_m(z+h) \sum_{n=-\infty}^{\infty} A_{mn_i} K_n(k_m r_i)\, e^{in\theta_i}. \tag{2.1}$$

Here $H_n^{(1)}$, K_n are respectively the nth-order Hankel functions of the first kind and modified Bessel functions of the second kind, and the wavenumbers k_0, k_m, $m = 1, 2, \ldots$, are the positive real roots of the dispersion equations

$$k_0 \tanh k_0 h = \omega^2/g, \tag{2.2a}$$

and

$$k_m \tan k_m h = -\omega^2/g, \quad (m = 1, 2, \ldots), \tag{2.2b}$$

for water depth h and gravitational acceleration g. In (2.1), A_{mn} are unknown complex amplitudes to be determined, and the first and second terms represent the

† The derivation for the radiation problem follows closely the development here and will not be elaborated.

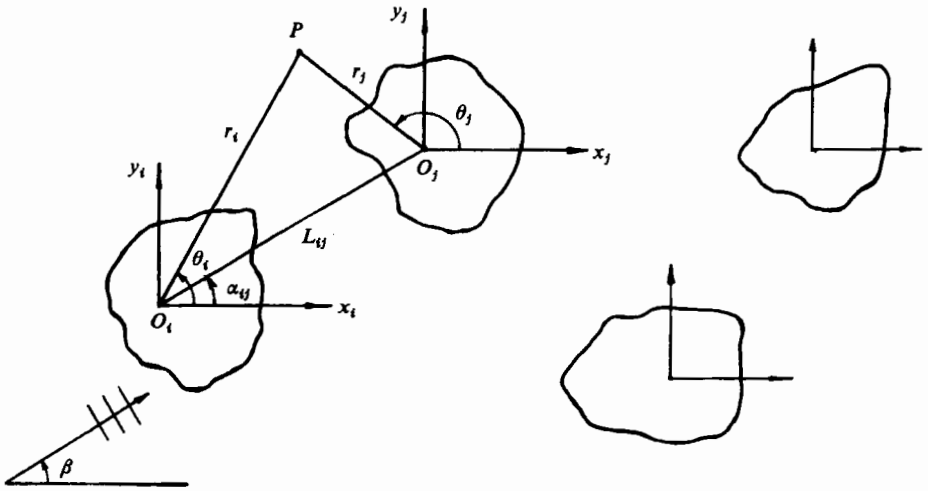

FIGURE 1. Definition sketch for a multiple-member body (plan view).

propagating and evanescent wavefields respectively. For brevity we adopt a matrix notation for (2.1),

$$\phi_i^{\mathrm{S}} = \boldsymbol{A}_i^{\mathrm{T}} \boldsymbol{\Psi}_i^{\mathrm{S}}(r_i, \theta_i, z), \tag{2.3}$$

where here and in the sequel a suitable truncation is always implied, and $\boldsymbol{A}_i$, $\boldsymbol{\Psi}_i^{\mathrm{S}}$ are respectively the vectors of coefficients A_{mn} and the scattered cylindrical partial waves in terms of $H_n^{(1)}$ and K_n.

To account for interactions among the bodies, it is necessary to evaluate the scattered potential ϕ_i^{S} in terms of the representation of the incident potential ϕ_j^{I} at body $j, j = 1, 2, \ldots, N, j \neq i$. This can be accomplished by the addition theorems for Bessel functions (Abramowitz & Stegun 1964), valid for $r_j < L_{ij}$;

$$H_n^{(1)}(k_0 r_i)\, \mathrm{e}^{\mathrm{i}n(\theta_i - \alpha_{ij})} = \sum_{l=-\infty}^{\infty} H_{n+l}^{(1)}(k_0 L_{ij})\, J_l(k_0 r_j)\, \mathrm{e}^{\mathrm{i}l(\pi - \theta_j + \alpha_{ij})},$$

$$(i, j = 1, 2, \ldots, N, \quad i \neq j), \tag{2.4a}$$

and

$$K_n(k_m r_i)\, \mathrm{e}^{\mathrm{i}n(\theta_i - \alpha_{ij})} = \sum_{l=-\infty}^{\infty} K_{n+l}(k_m L_{ij})\, I_l(k_m r_j)\, \mathrm{e}^{\mathrm{i}l(\pi - \theta_j + \alpha_{ij})}$$

$$(i, j = 1, 2, \ldots, N, \quad i \neq j), \tag{2.4b}$$

where L_{ij} is the distance between the origins O_i and O_j, α_{ij} the azimuthal angle of O_j relative to O_i (see figure 1) and J_l, I_l are respectively the Bessel and modified Bessel functions of the first kind of order l. (In addition to the requirement of non-overlapping vertical projections, the restriction $r_j < L_{ij}$ in essence further requires, for non-axisymmetric bodies, that the escribed cylinder to each body centred at its respective origin must not enclose any other origin.) Equations (2.4) define a coordinate transformation $\boldsymbol{T}_{ij}$ from i to j representation for the set of partial waves:

$$\boldsymbol{\Psi}_i^{\mathrm{S}} = \boldsymbol{T}_{ij} \boldsymbol{\Psi}_j^{\mathrm{I}}, \tag{2.5}$$

where $\boldsymbol{\Psi}_j^{\mathrm{I}}$ is the vector of *incident* partial-wave functions represented by J_n and I_n. Comparing (2.4) and (2.5), we note that the elements of $\boldsymbol{T}_{ij}$ are of the form

$$(\boldsymbol{T}_{ij})_{pq} = \mathrm{e}^{\mathrm{i}(q-p)\alpha_{ij}} H^{(1)}_{q-p}(k_o L_{ij}) \tag{2.6a}$$

for the propagating ($m = 0$) modes, and

$$(\boldsymbol{T}_{ij})_{pq} = \mathrm{e}^{\mathrm{i}(q-p)\alpha_{ij}}(-1)^{p-1} K_{q-p}(k_m L_{ij}) \tag{2.6b}$$

for the evanescent ($m > 0$) modes.

Substituting (2.5) into (2.3), the potential ϕ_i^{S} evaluated in terms of the wavefield at j is

$$\phi_i^{\mathrm{S}}|_j = \boldsymbol{A}_i^{\mathrm{T}} \boldsymbol{T}_{ij} \boldsymbol{\Psi}_j^{\mathrm{I}}. \tag{2.7}$$

The total incident potential in the vicinity of body j due to the scattering of all the other bodies and the ambient incident field ϕ_0 is thus

$$\begin{aligned}\phi_j^{\mathrm{I}} &= \phi_0|_j + \sum_{\substack{i=1 \\ i\neq j}}^{N} \boldsymbol{A}_i^{\mathrm{T}} \boldsymbol{T}_{ij} \boldsymbol{\Psi}_j^{\mathrm{I}} \\ &= \left(\boldsymbol{a}_j^{\mathrm{T}} + \sum_{\substack{i=1 \\ i\neq j}}^{N} \boldsymbol{A}_i^{\mathrm{T}} \boldsymbol{T}_{ij}\right) \boldsymbol{\Psi}_j^{\mathrm{I}}, \quad (j = 1, 2, \ldots, N).\end{aligned} \tag{2.8}$$

where $\boldsymbol{a}_j$ is simply the coefficient vector of the partial-wave decomposition of ϕ_0 about O_j, and $(\boldsymbol{a}_j)_p \neq 0$ only for propagating modes p.

Finally, we observe that the total incident and scattered waves for any body j ((2.8) and (2.3)) must be related by the (isolated-body) diffraction characteristics of that body. Specifically, there exist 'diffraction transfer matrices' $\boldsymbol{B}_j$ (often also referred to as T-matrices) for bodies $j = 1, 2, \ldots, N$ that relate the incident and diffracted partial waves at j, i.e.

$$\boldsymbol{A}_j = \boldsymbol{B}_j\left(\boldsymbol{a}_j + \sum_{\substack{i=1 \\ i\neq j}}^{N} \boldsymbol{T}_{ij}^{\mathrm{T}} \boldsymbol{A}_i\right), \quad (j = 1, 2, \ldots, N). \tag{2.9}$$

Thus element $(\boldsymbol{B}_j)_{pq}$ is the amplitude of the pth partial wave of the scattered potential due to a single unit-amplitude incidence of mode q on body j. For general geometries, the transfer matrix $\boldsymbol{B}_j$ is fully populated. When the body is axisymmetric, however, $\boldsymbol{B}_j$ is sparse owing to the circular-cylindrical decomposition of (2.1), and the result is simplified.

In an interaction theory we simply assume that the $\boldsymbol{B}_j$ are given from single-body diffraction calculations (or experiments), so that (2.9) can be solved for the unknown amplitudes $\boldsymbol{A}_i$. Once these amplitudes are determined, the primary forces and moments and the second-order drift forces on each body can be calculated directly by integrating over individual body surfaces (the single body diffraction analysis must also provide body potentials corresponding to each outer partial wave mode). Results for the entire structure can be obtained by summing, and for the steady horizontal drift forces alternatively by accounting for the total momentum change in the far field (Newman 1967). The far-field approach is particularly convenient when the number N of bodies is large, although care must be exercised to re-express the diffraction potentials ϕ_i^{S}, $i = 1, 2, \ldots, N$ in a common coordinate system.

3. Single-body diffraction – Determination of B – for an axisymmetric geometry

For simplicity, we consider only the case where the body is axisymmetric with respect to O. Because of the inclusion of evanescent modes, the diffraction transfer matrix $\boldsymbol{B}$ contains terms corresponding to the following two diffraction problems.

(i) *Scattering of a progressive incident mode*

$$\phi^{\mathrm{P}}_{\mathrm{I}n} = \frac{\cosh k_0(z+h)}{\cosh k_0 h} J_n(k_0 r)\, \mathrm{e}^{\mathrm{i}n\theta}, \quad (n = 0, \pm 1, \pm 2, \ldots), \tag{3.1a}$$

with the resulting far-field scattered wave

$$\phi^{\mathrm{P}}_{\mathrm{S}n} = C^{\mathrm{P}}_{0n} \frac{\cosh k_0(z+h)}{\cosh k_0 h} H^{(1)}_n(k_0 r)\, \mathrm{e}^{\mathrm{i}n\theta} + \sum_{m=1}^{\infty} C^{\mathrm{P}}_{mn} \cos k_m(z+h)\, K_n(k_m r)\, \mathrm{e}^{\mathrm{i}n\theta},$$
$$(n = 0, \pm 1, \pm 2, \ldots). \tag{3.1b}$$

(ii) *Scattering of an evanescent incident mode*

$$\phi^{\mathrm{L}}_{\mathrm{I}ln} = \cos k_l(z+h)\, I_n(k_l r)\, \mathrm{e}^{\mathrm{i}n\theta}, \quad (l = 1, 2, \ldots, \quad n = 0, \pm 1, \pm 2, \ldots), \tag{3.2a}$$

with the corresponding far-field scattered potential

$$\phi^{\mathrm{L}}_{\mathrm{S}ln} = C^{\mathrm{L}}_{l0n} \frac{\cosh k_0(z+h)}{\cosh k_0 h} H^{(1)}_n(k_0 r)\, \mathrm{e}^{\mathrm{i}n\theta} + \sum_{m=1}^{\infty} C^{\mathrm{L}}_{lmn} \cos k_m(z+h)\, K_n(k_m r)\, \mathrm{e}^{\mathrm{i}n\theta}$$
$$(l = 1, 2, \ldots, \quad n = 0, \pm 1, \pm 2, \ldots). \tag{3.2b}$$

Note that (i) is typically encountered in plane (progressive) wave diffraction (after partial-wave decomposition), while (ii) corresponds to a somewhat fictitious problem of diffraction of a (spatially) monotonic disturbance characterized by I_n. Both sets of potentials (3.1) and (3.2) satisfy the classical linearized boundary-value problem for an axisymmetric body. For $\phi_n = \phi_{\mathrm{I}n} + \phi_{\mathrm{S}n} = \varphi_n\, \mathrm{e}^{\mathrm{i}n\theta}$

$$\left(\frac{1}{r}\frac{\partial}{\partial r}\left(r\frac{\partial}{\partial r}\right) - \frac{n^2}{r^2} + \frac{\partial^2}{\partial z^2}\right)\varphi_n = 0 \quad \text{in the fluid } V,\ z < 0, \tag{3.3a}$$

$$\left(\frac{\partial}{\partial z} - \frac{w^2}{g}\right)\varphi_n = 0 \quad \text{on the free-surface } F,\ z = 0, \tag{3.3b}$$

$$\frac{\partial \varphi_n}{\partial n} = 0 \quad \text{on the body and bottom}, \tag{3.3c}$$

and a suitable radiation condition holds for the scattered part of φ_n (see (3.1*b*), (3.2*b*)).

Equations (3.3*a–c*) are solved for the unknown coefficients C^{P}_{0n}, C^{P}_{mn}, C^{L}_{l0n} and C^{L}_{lmn} ($l, m = 1, 2, \ldots$ and $n = 0, \pm 1, \pm 2, \ldots$), which are the elements of $\boldsymbol{B}$. We remark that if evanescent waves are ignored in the interaction, $\boldsymbol{B}$ contains only C^{P}_{0n}, $n = 0, \pm 1, \pm 2, \ldots$, and only problem (i) is required.

When the body is a uniform vertical cylinder that spans the water depth, (3.1) and (3.2) can be extended to the body surface, and the coefficients C^{P}, C^{L} are given analytically from the separable equations (3.3). In general, however, one must resort to numerical solutions for the two-dimensional (axisymmetric) propagating and evanescent wave diffraction problems. While a number of reliable diffraction techniques are now available (Mei 1978) (strictly only for problem (i)), we develop an axisymmetric hybrid-element method which is based on a variational formulation

using a finite-element discretization near the body and an analytic series representation outside a vertical circular cylinder enclosing the body. This approach is a particularly attractive alternative since in this case the outer representations are precisely of the form (3.1*b*) and (3.2*b*) for the progressive and local wave diffraction problems respectively. The details of the axisymmetric hybrid element method is very similar to that of Yue *et al.* (1978) for three-dimensional problems, and an outline is given in the Appendix for convenience.

Once the diffraction matrices $\boldsymbol{B}_i$, for bodies $i = 1, 2, \ldots, N$ (if not identical), are completed, (2.9) can be solved for the total N-body solution for any arbitrary configuration of these bodies.

4. Results and discussion

To confirm the validity of the present method, and to investigate the effects of hydrodynamic interaction and the importance of local waves, the interaction theory of §§2 and 3 is implemented and applied to a number of configurations. For comparison, 'exact' diffraction computations are also performed using a three-dimensional hybrid-element method (HEM)† (Yue *et al.* 1978) which solves the flow for the complete structure so that full hydrodynamic interactions are modelled.

For computations, the infinite series in (2.1) are truncated to M evanescent modes ($m = 1, 2, \ldots, M$) and N_m angular components ($n = 0, \pm 1, \pm 2, \ldots, \pm N_m$) for $m = 0, 1, 2, \ldots, M$. The same truncations are also carried out for (2.4), (3.1) and (3.2). Assuming an identical choice for each body, the total number of unknowns for the problem is then

$$N_{\mathrm{T}} = N \sum_{m=0}^{M} (2N_m + 1).$$

Because of the disparate asymptotic behaviours of the various Bessel functions, we find it extremely important in the numerical scheme to properly normalize all these special functions with respect to both order and argument. The analysis is fairly standard and will be skipped here.

We consider here four different geometries, each consisting of N identical legs. The legs are vertical circular cylinders (or cylindrical segments) with (waterplane) radius a (diameter $D = 2a$) and (total) draft H. All our results are for the combined structure and are non-dimensionalized by:

$$F_i = \text{exciting force}/\rho g \pi a H a_0 N, \tag{4.1a}$$

$$M_{ij} = \text{added mass}/\rho \pi a^2 H N, \tag{4.1b}$$

$$N_{ij} = \text{wave damping}/\omega \rho \pi a^2 H N, \tag{4.1c}$$

$$\bar{F}_i = \text{steady drift force}/\rho g \pi a a_0^2 N. \tag{4.1d}$$

Here ρ is the fluid density, a_0 the ambient incident wave amplitude, and $i, j = 1, 2, \ldots, 6$ the generalized coordinates (for surge, sway, ..., yaw). For moments and rotations ($i, j > 3$) the origin is always fixed on the free-surface at the centre of the total structure, and the normalizations (4.1) contain the extra length factor(s) a. In the following, h is the water depth, L the centre-to-centre spacing between the legs, and the incident wave angle β is measured from the x-axis (figure 1).

† A recent study (Matsui & Kato 1983) has found that for a variety of geometries (where analytic results are available), HEM yields somewhat better efficiency and accuracy than the classical boundary-integral equation (singularity-distribution) method.

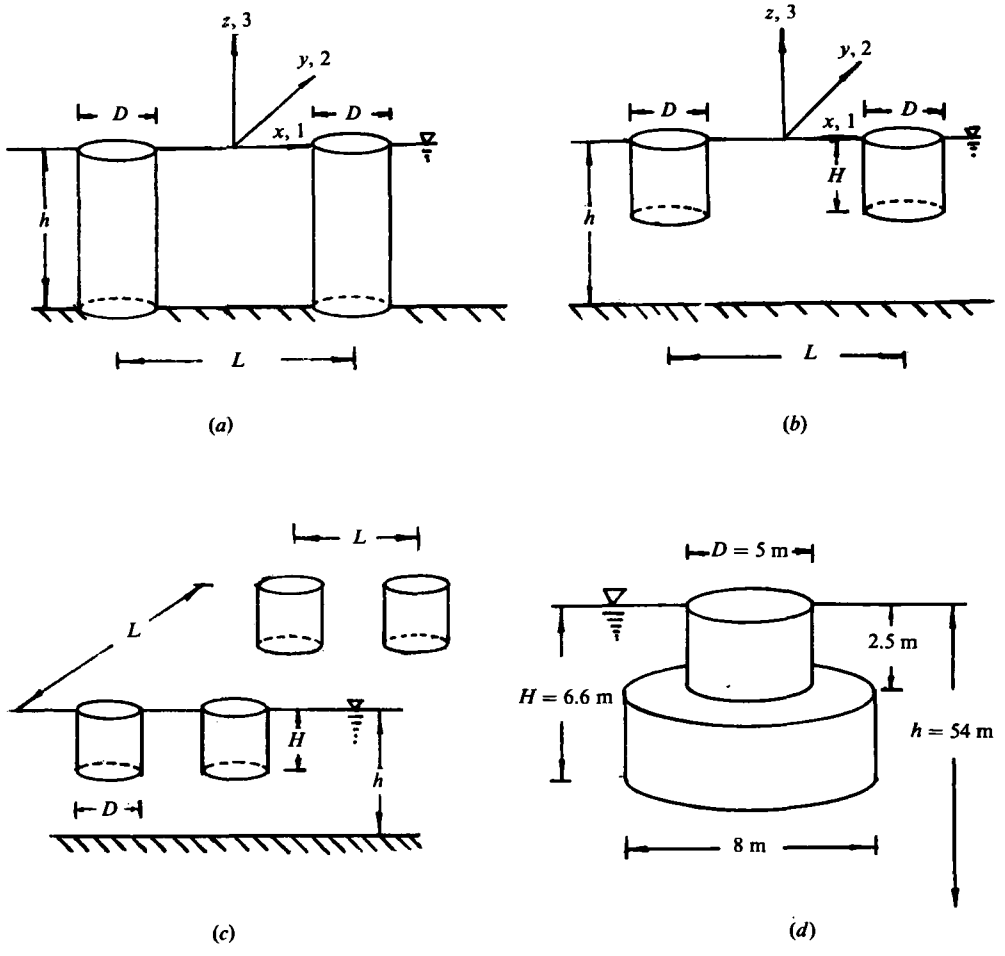

FIGURE 2. Geometries for: (*a*) two uniform (bottom-seated) vertical cylinders; (*b*) two truncated (floating) vertical cylinders; (*c*) four truncated (floating) vertical cylinders; (*d*) a composite cylindrical leg of a 3 by 11 floating array.

Geometry 1. *Two uniform* (*bottom-seated*) *vertical cylinders* (*figure* 2*a*)

To evaluate the influence of local waves, two spacings $L/D = 2$ and 4 with a fixed depth of $h/D = 2$ are considered. For this geometry the diffraction matrix $\boldsymbol{B}$ for a single body can be obtained analytically, and evanescent effects ($A_{mn}, m > 0$ in (2.1) and ϕ^{L} of (3.2)) are present only for the radiation (forced-motion) problems.

Figure 3 shows sample results† for the narrower spacing ($L/D = 2$) plotted against non-dimensional wavenumber $k_0 D$. For every case, including second-order forces, the present interaction theory agrees almost exactly with the full diffraction (HEM) results. For the interaction calculation $N_{\mathrm{T}} = 18$ complex unknowns ($M = 0$, $N_0 = 4$, no local waves) for the diffraction problems (exciting and drift forces) and $N_{\mathrm{T}} = 54$ ($M = 2$, $N_m = 4$ for $m = 0, 1, 2$, including local wave interaction) for the radiation problems are used. In contrast, the HEM computations, which utilize two vertical

† For all the configurations considered in this paper, computations and comparisons have been made for all the degrees of freedom and for a range of incident angles. Owing to space considerations, only representative results are shown.

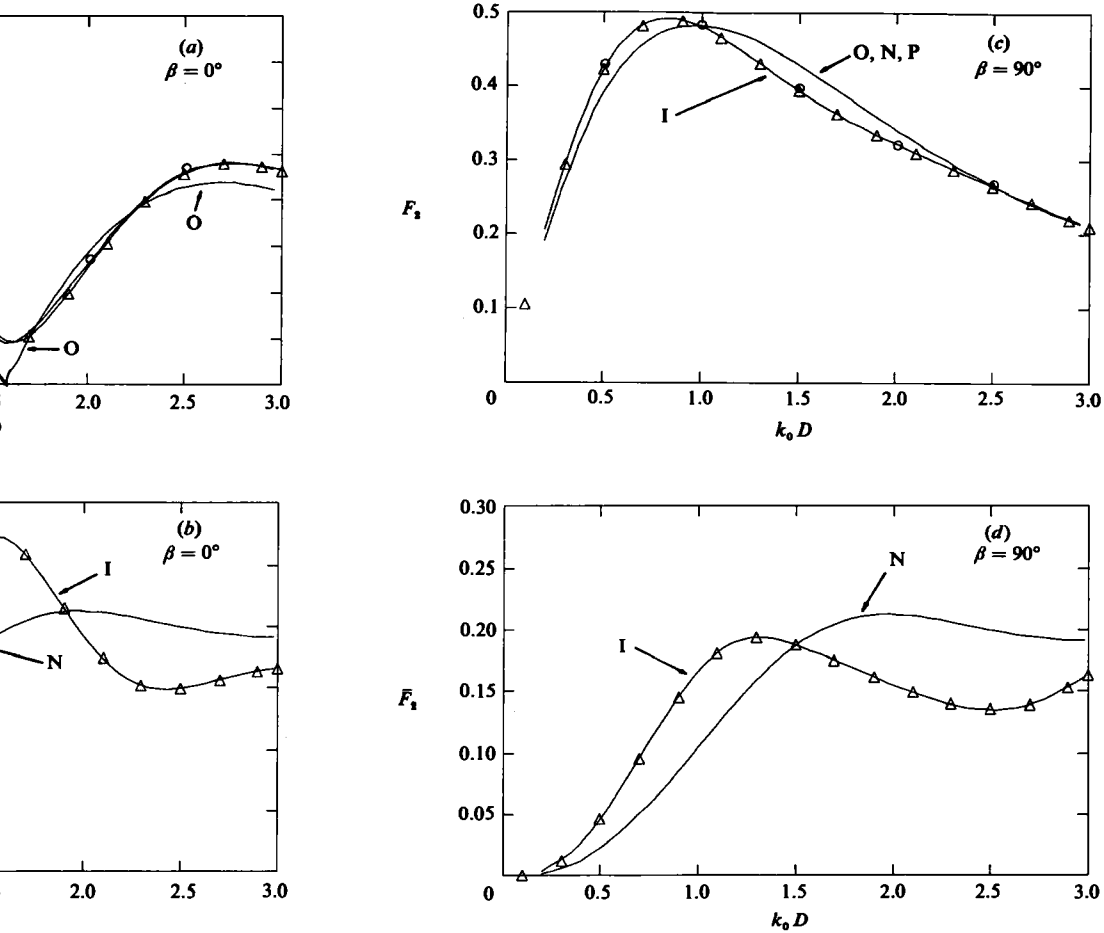

form vertical cylinder geometry of $h/D = 2$, $L/D = 2$ for: △, full diffraction (HEM) calculation; (curves) g local waves; L, interaction theory including local waves; N, no interaction (single-body) prediction; O, zeroth-order theory based on phasing only; P, plane-wave approximation; ○, plane-wave er & Evans' (1984) correction.

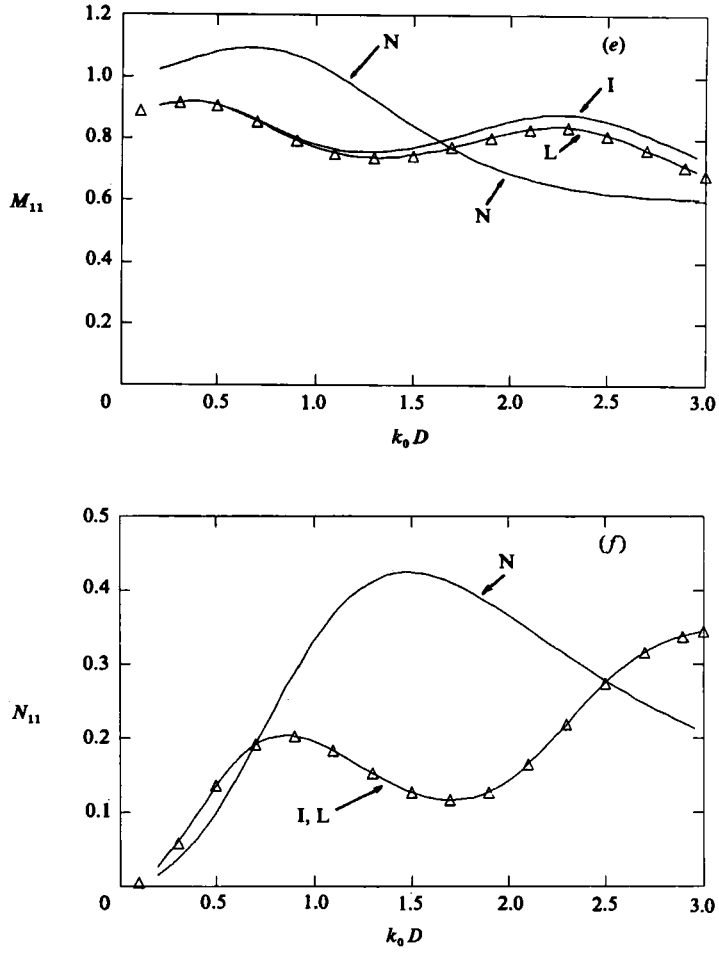

FIGURE 3(*e*, *f*). For caption see facing page.

	F_x	$\bar{F}_x$
HEM	0.2310	0.1662
interaction theory ($M = 0$)		
$N_0 = 2$ ($N_T = 10$)	0.2290	0.1650
$N_0 = 4$ ($N_T = 18$)	0.2314	0.1667
$N_0 = 7$ ($N_T = 30$)	0.2314	0.1667

TABLE 1. Typical convergence of interaction-theory results for the case of two uniform legs $L/D = 2$, $h/D = 2$, $k_0 D = 3$.

planes of symmetry and an optimal elliptical analytic matching boundary (owing to the elongated two-body configuration), require 483 complex unknowns (453 quadratic element nodes and 30 far-field coefficients) for a comparable accuracy of less than $\sim 1\,\%$ error. Some typical interaction theory convergence figures are given in table 1.

Returning to figure 3, we see that for the surge-exciting-force magnitude $F_1(\beta = 0°)$

(figure 3*a*), a zeroth-order theory (i.e. one that only accounts for the incident wave phasing at the individual legs),

$$F_1(\beta)_{\text{0th-order}} = \cos(\tfrac{1}{2}k_0 L\cos\beta)\, F_{1\,\text{single leg}}, \tag{4.2}$$

already produces rather reasonable results. For comparison, F_1 obtained using a 'plane-wave' approximation similar to that of Simon (1982) as well as the improved method of McIver & Evans (1984) are also shown for the primary exciting forces. The interaction effect is much more interesting for the steady drift force (figure 3*b*), where the prediction based on a single leg (neglecting all interactions) is clearly inadequate.

In beam seas ($\beta = 90°$) the first-order force F_2 (figure 3*c*) deviates only slightly from the zeroth-order approximation. Note that for $\beta = 90°$ both the zeroth-order and 'plane-wave' approximations reduce identically to the single body (no interaction) result, whereas the interaction is captured quite well by the McIver & Evans correction. In contrast with F_2, the steady drift force $\bar{F}_2$ (figure 3*d*) still exhibits a rather pronounced effect of interaction. Calculations have also been performed for oblique incident waves ($0° < \beta < 90°$) with equally satisfactory comparisons. The results are qualitatively similar to those of figures 3(*a*, *b*) and (*c*, *d*) for the surge and sway forces, and are not shown.

For the horizontal-radiation problems evanescent waves are present. Figure 3(*e*) shows the surge added-mass coefficient M_{11} for the two-leg structure. Observe that the present theory including local modes produces excellent agreement with 'exact' calculation, while when only the progressive waves are used the comparison is less satisfactory. The deviation and thus the contribution of local wave interaction, interestingly, is greater for short wavelengths and diminishes for long waves, contrary to that suggested by a 'wide-spacing' assumption based upon large $k_0 L$. For finite depth, evanescent wave amplitudes in general decrease exponentially at distance L with increasing $(L-a)/h$ for typical body dimension a, and depend only weakly on (increase with larger) $k_0 L$. This can be clarified by a simple analytic demonstration. Consider, for example, the swaying (with unit velocity) of a uniform vertical cylinder of radius a. The separable solution is simply

$$\phi(r,\theta,z) = \sum_{m=0}^{\infty} \phi_m(r,z)\cos\theta,$$

where
$$\phi_0(r,z) = \frac{2}{k_0^2 h}\frac{\sinh k_0 h\cosh k_0 h}{1+\sinh 2k_0 h/2k_0 h}\frac{H_1(k_0 r)}{H_1'(k_0 a)}$$

and
$$\phi_m(r,z) = \frac{2}{k_m^2 h}\frac{\sin k_m h\cos k_m(z+h)}{1+\sin 2k_m h/2k_m h}\frac{K_1(k_m r)}{K_1'(k_m a)}, \quad m = 1,2,\ldots. \tag{4.3}$$

For moderate values of $k_0 h$, $k_m h$ are close to $m\pi$ and are relatively insensitive to the frequency $\sigma = \omega^2 h/g$ (see (2.2*b*)):

$$k_m h = m\pi\left[1-\frac{\sigma}{(m\pi)^2}+O\left(\frac{\sigma}{(m\pi)^2}\right)^2\right]. \tag{4.4}$$

At a distance L the magnitude of the mth evanescent mode is (upon using the asymptotics for large argument for K) approximately

$$\phi_m|_{(r,z)=(L,0)} \sim \left(\frac{a}{L}\right)^{\frac{1}{2}}\frac{\sin 2k_m h}{k_m^2 h}\,\mathrm{e}^{-(k_m h)(L-a)/h}. \tag{4.5}$$

Comparing the magnitudes of ϕ_0 and ϕ_m on $z = 0$ where the ratio is minimum, we have (for $k_0 h > O(1)$)

$$\left.\frac{\phi_m}{\phi_0}\right|_{(r,z)=(L,0)} \sim \left(\frac{a}{L}\right)^{\frac{1}{2}} \frac{H_1'(k_0 a)}{H_1(k_0 L)} \frac{k_0 \sin 2k_m h}{2k_m^2 h} e^{-(k_m h)(L-a)/h}. \tag{4.6}$$

In general, then, for an axisymmetric body of (average) radius a, an estimate of the dominant dependence is

$$\phi_m|_L \sim e^{-k_m h(L-a)/h}. \tag{4.7}$$

Thus for a fixed depth h, local waves can be ignored at adjacent bodies when the spacing is large compared with body dimension and water depth (specifically, $(L-a)/h \gg 1$). On the other hand, for a given configuration, $\phi_m|_L$ does not diminish for shorter (propagation) wavelengths, but in fact increases with frequency σ according to (4.4) and (4.7).

Finally, we show the surge damping coefficient N_{11} in figure 3(f). As expected, the inclusion of local waves has no effect on the damping coefficient, although a crude estimate based on a single leg is qualitatively incorrect. The coefficients for transverse motions (M_{22}, N_{22} etc.) exhibit similar but smaller interaction effects and are not shown.

Similar calculations have also been performed (but not shown here) for a wider spacing ($L/D = 4$) with equally excellent agreement between the interaction theory and exact diffraction predictions. With the larger L/D, the interaction features do not diminish significantly as compared with figure 3, but exhibit more rapid variations (cf. (4.2)). The drift force $\bar{F}_1$ shows a decaying oscillation with $k_0 D$ about the single-leg result, both of which eventually approach the short-wave asymptotic value of $2/(3\pi)$ (Havelock 1940). The effect of local waves is now nearly negligible for the added mass, confirming the validity of ignoring these waves for larger inter-body spacings.

Geometry 2. *Two truncated vertical cylinders* (*figure* 2*b*)

The cylinders are now truncated at a draft $H = D$ floating in water of depth $h = 2D$. Unlike the preceding example, evanescent waves are present for both diffraction and radiation. There are no analytic solutions for the transfer matrices $\boldsymbol{B}$, and the progressive and local wave diffraction problems are calculated numerically as explained in §3. We have studied three different spacing ratios $L/D = 1.3$, 2 and 4; however, typical results are shown only for the smallest spacing $L/D = 1.3$ (figure 4). The interaction-theory results, which are based on numerical single-body coefficients, again give uniformly satisfactory comparisons with full diffraction calculations. For all the cases, we use $N_T = 54$ ($M = 2$, $N_m = 4$, $m = 0, 1, 2$) and $N_T = 18$ ($M = 0$, $N_0 = 4$) when we ignore local waves. HEM now requires between 700 and over 900 total unknowns, depending on spacing. An example of convergence for the present method with respect to both M and N and comparisons to HEM and single leg results for this geometry are shown in table 2.

For $L/D = 1.3$ the effect of local wave interaction on F_1 (figure 4a) is present mainly at the longer wavelengths. This is also true for N_{11} (figure 4b). For this geometry evanescent waves are introduced by the mismatch of boundary condition below $z = -H$, so that local wave amplitudes vanish rapidly with increasing $k_0 H$. The effects are smaller for drift force $\bar{F}_1$ (figure 4c) and affect only the very small wavenumbers. This can be seen from a pressure-integration expression for the drift surge force, where a large contribution comes from the waterline, while the quadratic term in the body

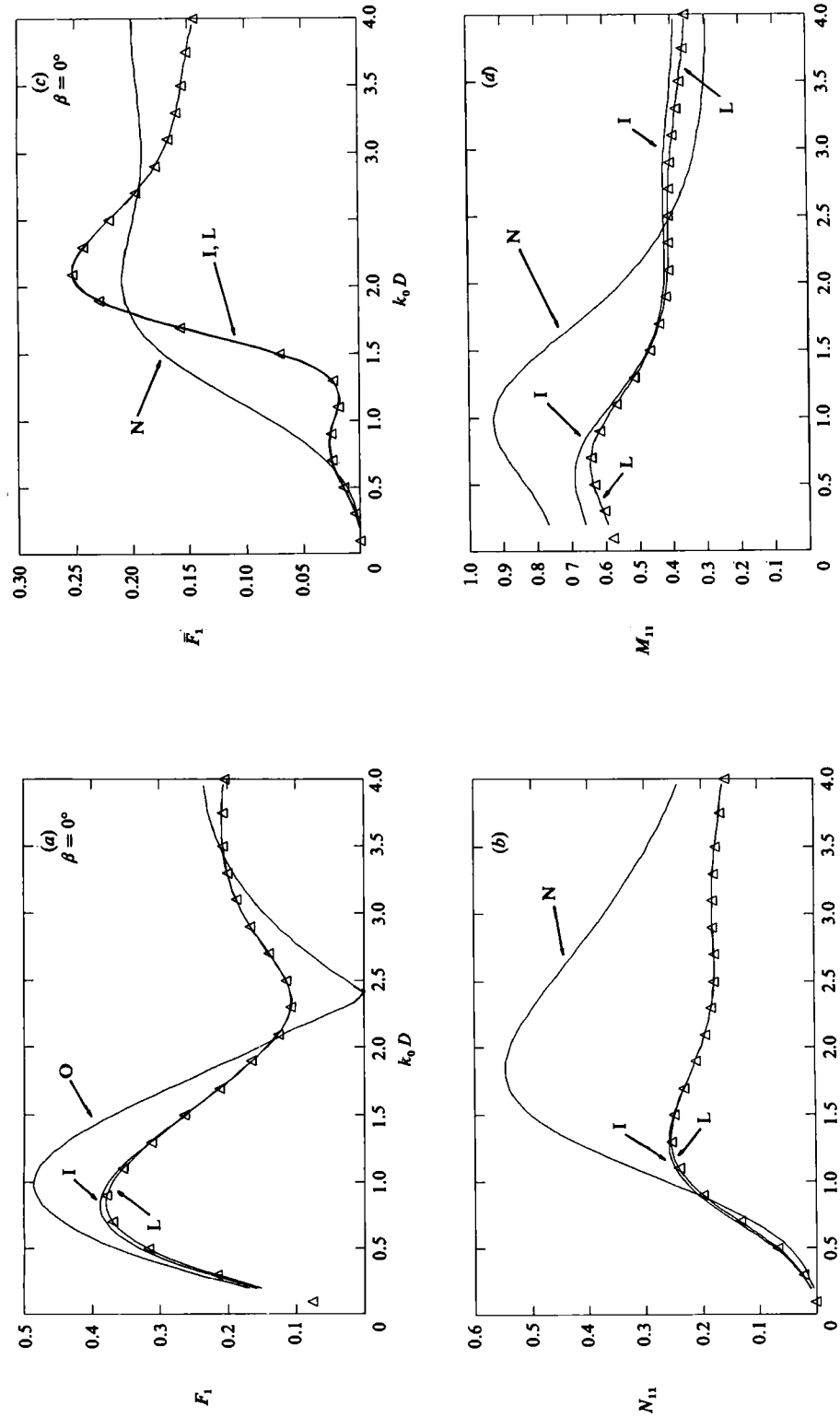

FIGURE 4. Results for a two truncated vertical cylinder geometry of $h/D = 2$, $H/D = 1$, $L/D = 1.3$ for: Δ, full diffraction (HEM) calculation; (curves) I, interaction theory neglecting local waves; L, interaction theory including local waves; N, no interaction (single-body) prediction; O, for primary exciting forces, zeroth-order theory based on phasing only.

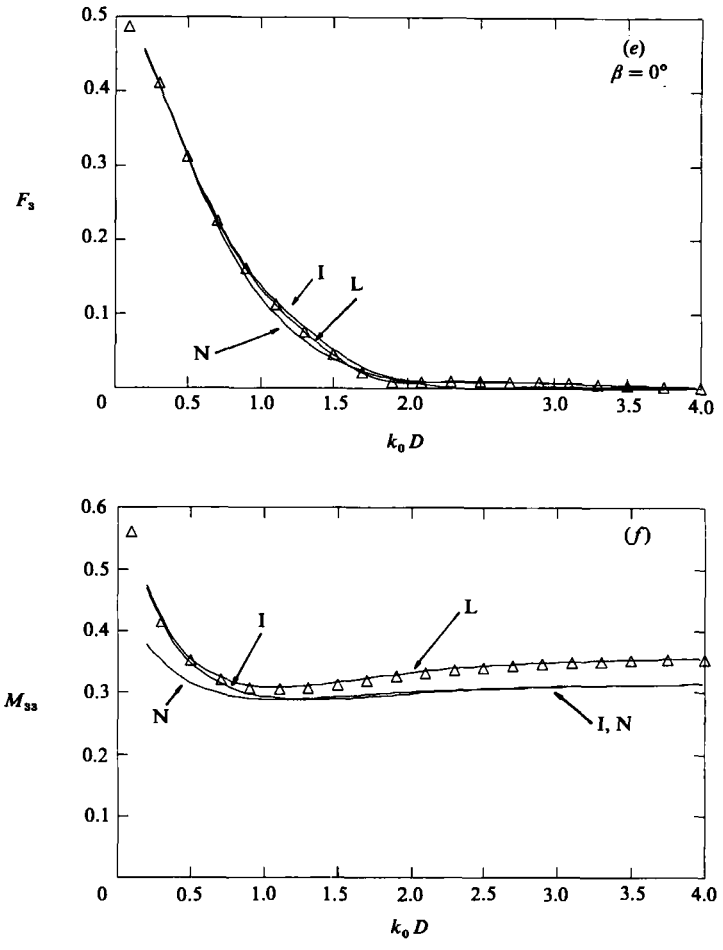

FIGURE 4(*e*, *f*). For caption see facing page.

	F_x	F_z	M_{11}	M_{33}	N_{11}	$\bar{F}_x$
Single body (no interaction)	—	—	0.32423	0.31054	0.35599	0.19124
Single body (with phasing)	0.16433	0.00363	—	—	—	—
HEM	0.18828	0.00779	0.39797	0.34852	0.18146	0.16736
Interaction theory						
$M = 0$ $N_0 = 4$	0.18871	0.00754	0.41866	0.31033	0.18164	0.16762
$M = 1$ $N_0 = 4$	0.18875	0.00777	0.41338	0.34694	0.18182	0.16763
$M = 2$ $N_0 = 2$	0.18848	0.00761	0.39405	0.35070	0.18403	0.17583
$N_0 = 4$	0.18879	0.00772	0.39739	0.35076	0.18185	0.16763
$N_0 = 7$	0.18880	0.00772	0.39740	0.35076	0.18185	0.16767
$M = 3$ $N_0 = 4$	0.18880	0.00772	0.39260	0.35160	0.18183	0.16763

TABLE 2. Typical convergence of interaction-theory results for the case of two truncated legs $L/D = 1.3$, $H = D$, $h = 2D$, $k_0 D = 3.1$

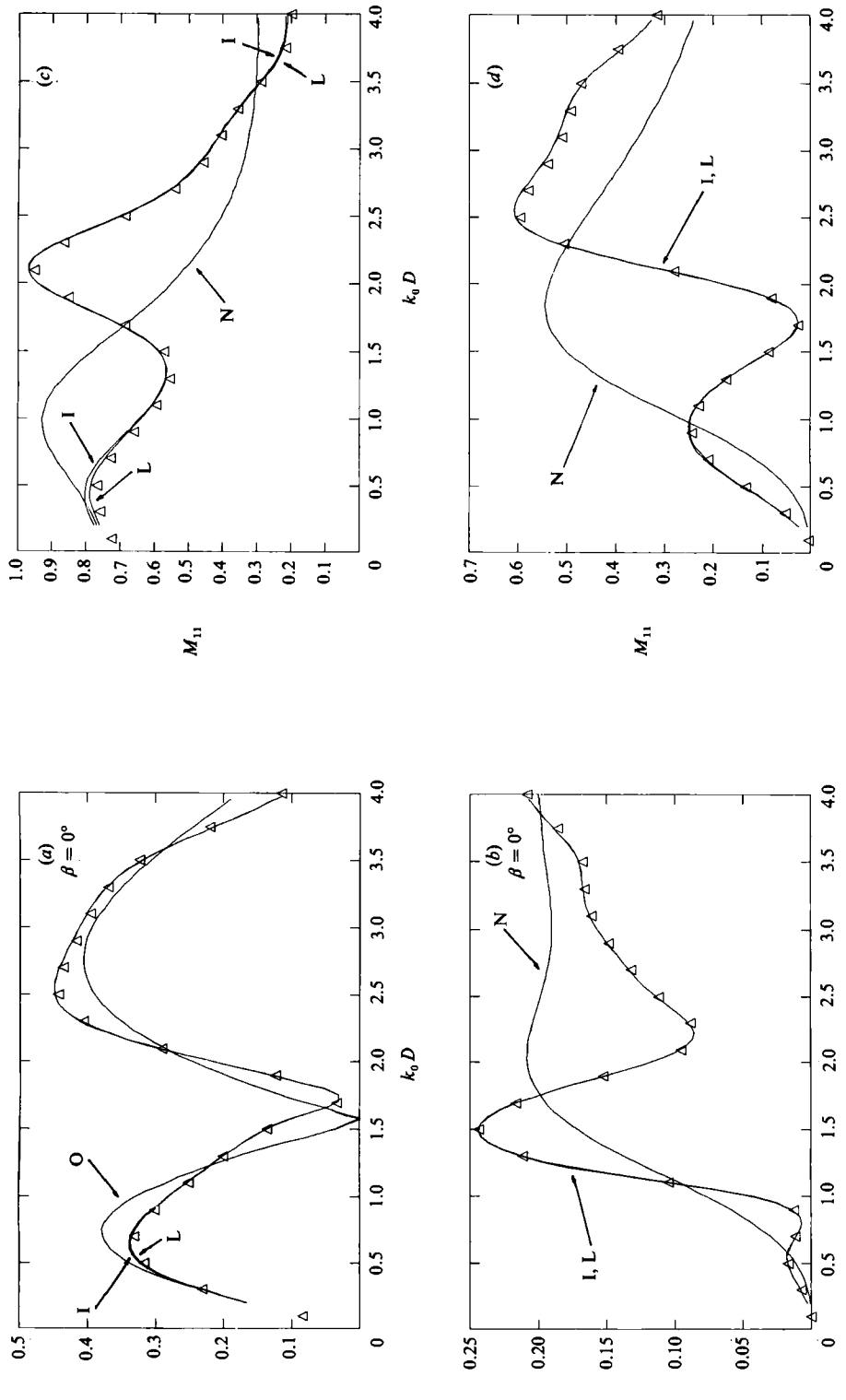

FIGURE 5. Results for a four truncated vertical cylinder geometry of $h/D = 2$, $H/D = 1$, $L/D = 2$ for: $\triangle$, full diffraction (HEM) calculation; (curves) I, interaction theory neglecting local waves; L, interaction theory including local waves; N, no interaction (single-body) prediction; O, for primary exciting forces, zeroth-order theory based on phasing only.

surface integral decays twice as rapidly with depth ($\sim e^{2k_0 z}$) as the incident potential. The situation is rather different for M_{11} (figure 4*d*), where predictions with or without evanescent waves differ in both the short- and long-wave ranges.

For vertical motions and forces, the effect of hydrodynamic interaction and of local wave diffraction is small for F_3 (figure 4*e*). For the added mass M_{33} (figure 4*f*), however, evanescent waves have a very distinct influence, especially for large $k_0 D$. The interaction curves, with and without including evanescent effects, approach each other at low frequency but deviate appreciably as the wavelength decreases. Indeed, for large $k_0 D$, the latter coincides with the values for a single cylinder (no interaction), while the inclusion of local waves in the former yields the correct results. Strictly speaking, since the propagating and evanescent waves interact with each other, one cannot conclude that evanescent waves only are responsible for interactions at high frequency. On the other hand, when the local wave components are kept but the amplitudes of all the propagating wave components are set to zero in the *final* expression for the incident wave at each body, we are able to recover essentially the earlier correct large-$k_0 D$ results. Computations have also been performed for other incident angles and radiation modes, where there are generally somewhat smaller effects of interaction.

For the wider spacings we computed ($L/D = 2, 4$), the comparisons remain excellent, although the evanescent-wave effects become quite unimportant, largely confirming the findings of earlier investigators. In summary, we find that local wave interaction effects are important only when L/D is relatively small, and when present appear primarily in two ways: free-surface effects in the low-frequency regime, which are manifest in all the results; and non-free-surface effects, which affect the added-mass prediction for short wavelengths.

Geometry 3. *Four truncated vertical cylinders* (*figure* 2*c*)

To evaluate the importance of interaction as the number of bodies increases, we study a geometry with four legs with $H/D = 1$, $h/D = 2$ and $L/D = 2$. Structures similar to this have been used as supports for large offshore platforms where interaction effects on first- and second-order wave forces are of significant interest.

The results are shown in figure 5. The interaction theory now employs $N_T = 108$ unknowns ($N = 4$, $M = 2$, $N_m = 4$, $m = 0, 1, 2$). The full diffraction HEM calculation for a quadrant of the structure (utilizing two planes of symmetry) uses over 800 degrees of freedom. Because of storage and computation limitations, the HEM grid we used is somewhat coarser than required, especially for the higher wavenumbers. We believe this to be the source of the discrepancies in figure 5, since the interaction-theory values have already converged.

Comparing figures 4 and 5, the results (normalized by N) for two and four legs are qualitatively quite similar. This can be explained from earlier two-leg findings for different incident angles, where interaction effects are found to be dominant primarily when there is sheltering of the leeward body.

Geometry 4. *A* 3 *by* 11 ($N = 33$) *array of vertical cylinders with footings*

To test the effectiveness of the present interaction theory for large structures, we consider as a final example this array of 33 floating legs. This structure forms a portion of the support for a proposed floating airport in Japan (Ando *et al.* 1983). For increased buoyancy, each leg is placed on top of a larger cylindrical footing as shown in figure 2(*d*) (in prototype dimensions). The rectangular interleg spacing of the array is 16.4 m. For this geometry a full diffraction calculation is clearly infeasible.

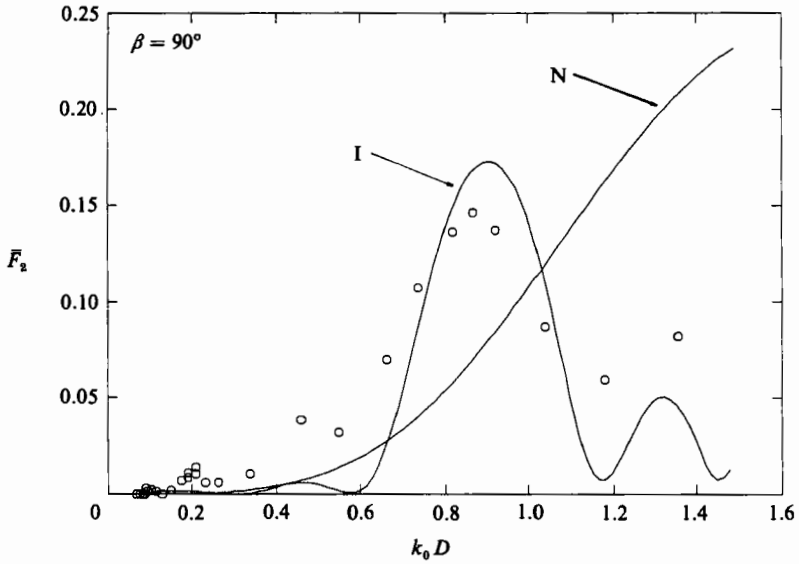

FIGURE 6. Results for a 33 (3 by 11) floating array of composite vertical cylindrical legs $D = 5$ m, $H = 6.6$ m, $h = 54$ m, $L = 16.4$ m for: ○, 1:30 scale experimental measurements; (curves) I, interaction theory (no local waves); N, no interaction (single-body) prediction.

However, a 1:30 scale experiment had been conducted earlier at the Offshore Structure Experimental Basin (40 × 27.6 m) of the Ship Research Institute of Japan by Kagemoto (1982). In that experiment the drift forces on the structure in regular beam waves were measured by using counterweights. The model was otherwise unconstrained (freely floating), although the amplitude of motion was small and measurable only for very long wavelengths. In the present calculation the hydrodynamics of a single composite-cylinder leg is obtained with the axisymmetrical diffraction code of §3, and the interaction theory is computed with a relatively small number of coefficients, $N_T = 165$ ($N = 33$, $M = 0$, $N_0 = 2$). Motions of the structure are neglected.

The result for the wave drift force $\bar{F}_2$ for incident waves in the transverse (3-leg) direction is given in figure 6. For comparison, the no-interaction (single-leg) prediction is also plotted. We can see that the effect of including interaction is significant, and the comparison of the interaction results with experimental data overall is fairly good.

For illustration we have made computations here for assemblies of identical axisymmetric bodies only. The method can be readily extended to non-identical or general-shaped bodies. The former is straightforward and involves calculating a different $\boldsymbol{B}$ for each different body geometry. The latter requires three-dimensional progressive and evanescent wave-diffraction computations for the single body (or bodies) to obtain the fully-populated $\boldsymbol{B}$-matrix (or matrices).

5. Summary

By combining and extending the matrix method of Simon (1982) and the multiple-scattering idea of Ohkusu (1974), an interaction theory has been developed which predicts the complete hydrodynamics of a multibody structure given only the diffraction characteristics of individual members. The present theory is in general applicable to any number, locations and geometries of bodies, which do not overlap

vertically, and when the evanescent wave system is retained, to arbitrary body spacings. When the bodies are not vertically axisymmetric, the use of addition theorems strictly requires that vertical circular cylinders can be constructed that enclose the individual bodies or interacting groups but do not contain the origin of another such cylinder. Possible extension of the present method to situations where this is violated is being investigated.

Numerical results have been given for a number of configurations of vertically axisymmetric bodies, where for comparison large-scale diffraction calculations for the entire structures have also been performed. The interaction theory gives almost exact predictions for first-order exciting forces, added-mass and damping coefficients and second-order steady drift forces. Local wave interaction is found to be important primarily for small spacing to body diameter ratios ($L/D \lesssim 2$) especially for added mass, and can sometimes be more appreciable for shorter wavelengths. A final example for a 3 by 11 array of floating bodies using only 165 coefficients shows a satisfactory comparison with experimental data, demonstrating the efficacy of the method.

When the detailed hydrodynamic properties of individual bodies or body groups are known, the present theory eliminates the need for full diffraction computations for a large class of multiple-body structures or arrays.

Financial support for this research was provided by the Fluid Mechanics program of the United States National Science Foundation (MEA-822210649). Portions of the computations reported here were performed on the NSF sponsored NCAR Cray computer. H. Kagemoto acknowledges the sponsorshop of the Science and Technology Agency of Japan for his year's leave at MIT. D. Yue also wishes to acknowledge partial support from the Henry L. Doherty Chair.

Appendix. Outline of the axisymmetric hybrid-element diffraction formulation

The diffraction of cylindrical progressing and local waves by an axisymmetic body is governed by (3.3). When the body geometry is irregular, analytic solutions cannot be found, and we enclose the body and a small fluid domain V around it by a fictitious vertical circular cylinder S. The boundary-value problem is now replaced by (3.3a–c) for φ_n inside S; (3.3a, b) and the radiation condition

$$\lim_{k_0 r \to \infty} r^{\frac{1}{2}}\left(\frac{\partial}{\partial r} - \mathrm{i}k_0\right)\varphi'_{Sn} = 0 \tag{A 1}$$

for the potential $\varphi'_n = \varphi'_{Sn} + \varphi_{In}$ outside S; and the matching conditions

$$\left.\begin{aligned} \varphi_n &= \varphi'_n && \text{(A 2}a\text{)} \\ \frac{\partial \varphi_n}{\partial r} &= \frac{\partial \varphi'_n}{\partial r} && \text{(A 2}b\text{)} \end{aligned}\right\} \quad \text{on } S.$$

If we now choose φ'_{Sn} to be given by (3.1b) or (3.2b) depending on φ_I, the combined boundary-value problem implies and is implied by the stationarity of the following functional (Yue *et al.* 1978):

$$J(\varphi_n, \varphi'_{Sn}) = \frac{1}{2}\int_V \left(\left(\frac{\partial \varphi_n}{\partial r}\right)^2 + \left(\frac{n\varphi_n}{r}\right)^2 + \left(\frac{\partial \varphi_n}{\partial z}\right)^2\right) \mathrm{d}V$$

$$-\frac{\omega^2}{2g}\int_F \varphi_n^2 \,\mathrm{d}F + \int_S \left(\left(\tfrac{1}{2}\varphi'_{Sn} - \varphi_{Sn}\right)\frac{\partial \varphi'_{Sn}}{\partial r} - \varphi_n \frac{\partial \varphi_{In}}{\partial r}\right)\mathrm{d}S. \tag{A 3}$$

The proof follows directly upon taking the first variation of J and using the fact that φ'_{Sn} satisfies (3.3a, b) and (A 1). Note that the matching conditions (A 2) are satisfied as *natural* boundary conditions by the variational principle (A 3).

In our hybrid-element implementation we truncate the series in (3.1b) or (3.2b) at $m = M$, and represent the potential φ_n in the (irregular) interior domain by 8-node isoparametric quadrilateral quadratic finite elements. Thus this approach takes advantage of the versatility of finite elements to describe complex geometries in a small inner region, and the power of analytic representation in the exterior infinite domain. Furthermore, because of the natural matching conditions, all of the unknown coefficients of φ'_{Sn} and nodal values of φ_n can be solved for simultaneously by a direct application of (A 3).

REFERENCES

Abramowitz, M. & Stegun, I. A. 1964 *Handbook of Mathematical Functions*. Government Printing Office, Washington.

Ando, S., Okawa, Y. & Ueno, I. 1983 Feasibility study of a floating offshore airport. *Rep. Ship Res. Inst. Suppl.* 4, *Tokyo* (in Japanese).

Budal, K. 1977 Theory for absorption of wave power by a system of interacting bodies. *J. Ship Res.* **21**, 241–253.

Duncan, J. H. & Brown, C. E. 1982 Development of a numerical method for the calculation of power absorption by arrays of similar arbitrarily shaped bodies in a seaway. *J. Ship Res.* **26**, 38–44.

Greenhow, M. J. L. 1980 The hydrodynamic interactions of spherical wave-power devices in surface waves. In *Power from Sea Waves* (ed. B. M. Count), pp. 287–343. Academic.

Havelock, T. H. 1940 The pressure of water waves upon a fixed obstacle. *Proc. R. Soc. Lond.* A **175**, 409–421.

Heaviside, O. 1950 *Electromagnetic Theory*, §182. Dover.

Kagemoto, H. 1982 The drift force on offshore structures. *Internal Rep. Ship Res. Inst. Tokyo* (in Japanese).

Kyllingstad, A. 1984 A low-scattering approximation for the hydrodynamic interactions of small wave-power devices. *Appl. Ocean Res.* **6**, 132–139.

Lebreton, J. C. & Cormault, P. 1969 Wave action on slightly immersed structures, some theoretical and experimental considerations. In *Proc. Symp. Wave Action*. 9, Paper 12A.

McIver, P. 1984 Wave forces on arrays of floating bodies. *J. Engng. Maths* **18**, 273–285.

McIver, P. & Evans, D. V. 1984 Approximation of wave forces on cylinder arrays. *Appl. Ocean Res.* **6**, 101–107.

Martin, P. A. 1984 Multiple scattering of surface water waves and the null-field method. In *Proc. 15th Symp. Naval Hydrodynamics*, pp. 119–132.

Matsui, T. & Kato, K. 1983 Computation of wave drift forces on floating axisymmetric bodies in regular waves. *Mem. Fac. Engng. Nagoya Univ.* **35**, 117–130.

Mei, C. C. 1978 Numerical methods in water-wave diffraction and radiation. *Ann. Rev. Fluid Mech.* **10**, 393–416.

Newman, J. N. 1967 The drift force and moment on ships in waves. *J. Ship Res.* **11**, 51–60.

Ohkusu, M. 1974 Hydrodynamic forces on multiple cylinders in waves. In *Proc. Intl. Symp. on Dynamics of Marine Vehicles and Structures in Waves, London*, Paper 12, pp. 107–112.

Simon, M. J. 1982 Multiple scattering in arrays of axisymmetric wave-energy devices. Part 1. A matrix method using a plane-wave approximation. *J. Fluid Mech.* **120**, 1–25.

Spring, B. H. & Monkmeyer, P. L. 1974 Interaction of plane waves with vertical cylinders. In *Proc. 14th Intl. Conf. on Coastal Engineering*, Chap. 107, pp. 1828–1845.

Srokosz, M. A. & Evans, D. V. 1979 A theory for wave-power absorption by two independently oscillating bodies. *J. Fluid Mech.* **90**, 337–362.

TWERSKY, V. 1952 Multiple scattering of radiation by an arbitrary configuration of parallel cylinders. *J. Acoust. Soc. Am.* **24**, 42–46.

WANG, S. & WAHAB, R. 1970 Heaving oscillations of twin cylinders in a free surface. *J. Ship Res.* **15**, 33–48.

YUE, D. K. P., CHEN, H. S. & MEI, C. C. 1978 A hybrid element method for diffraction of water waves by three-dimensional bodies. *Intl. J. Numer. Meth. Engng.* **12**, 245–266.